Materials Science-Poland, Vol. 24, No. 1, 2006

Structural, thermal and electrical properties of lithium–manganese spinel with a sulphur-substituted oxygen sublattice

M. MOLENDA[1], R. DZIEMBAJ[1,2*], A. KOTWICA[1], W. ŁASOCHA[1]

[1]Faculty of Chemistry, Jagiellonian University, ul. Ingardena 3, 30-060 Cracow, Poland

[2]Regional Laboratory of Physicochemical Analyses and Structural Research, ul. Ingardena 3, 30-060 Cracow, Poland

Sulphur substituted $LiMn_2O_{4-y}S_y$ spinels were obtained using the sol-gel method followed by calcination at 300 °C. The crystallinity of the samples was improved by further calcination at 800 °C. The monophase system was formed up to $y = 0.20$. At higher sulphur concentrations an additional phase (Mn_2O_3) appeared. The sulphided spinels were thermally stable in air up to about 900 °C. They decomposed above this temperature, with the oxidation of sulphur to SO_2. The decomposition products, $LiMnO_2$ and Mn_3O_4, reacted during slow cooling and formed stoichiometric $LiMn_2O_4$. Sulphur substitution retarded the phase transition at room temperature, although a new one appeared at higher temperatures (540–580 °C). Such an effect does not exist in sulphur-free spinels.

Key words: *oxysulphide spinel; sol-gel method; Li-ion battery; thermal stability*

1. Introduction

Lithium–manganese spinels, due to their economical and environmental friendly properties, are still of interest for lithium-ion battery developers [1, 2]. In the last decade, a large number of papers have been devoted to Li–Mn–O spinel systems as new cathodes for Li-ion batteries. Such an electrode, however, exhibits capacity fading during cell cycling. This is usually related to the structural instability of the cathode material [1, 3]. Stoichiometric $LiMn_2O_4$ spinel shows a reversible low-temperature phase transition from a cubic (*Fd*3*m*) to an orthorhombic (*Fddd*) structure near room temperature [4]. This phase transition is related to the Jahn–Teller distortion of Mn^{3+} ions [5, 6]. Structural stabilisation may be achieved by partially substitution Mn^{3+} ions

*Corresponding author, e-mail: dziembaj@chemia.uj.edu.pl

by *3d* metal ions (Cr, Fe, Ni, Co) [7, 8], Al^{3+} [9] ions, or excess of Li^{+} ions [10, 11]. These modifications, however, result in a decrease of the Mn^{3+}/Mn^{4+} ratio due to the substitution and/or charge compensation of the crystal lattice. This causes a remarkable decrease in 4 V capacity. In a recent paper, we have stressed that the appearance of the low-temperature phase transition is restricted to high-spin Mn^{3+} ions at high symmetric octahedral sites O_h [12] and to specific charge ordering in the manganese sublattice [4, 13].

The aim of this paper is to show the influence of isoelectronic substitution in the oxygen sublattice by sulphur on the structural and thermal stability of lithium–manganese spinels. Yang-Kook Sun et al. have reported an improvement in the cycling properties for lithium–manganese spinels doped with aluminium and sulphur ($LiAl_xMn_{2-x}O_{4-y}S_y$) in the 4 V region even at elevated temperatures [14–16]. Additionally, they found that these materials were more stable and less soluble in electrolytes than stoichiometric $LiMn_2O_4$.

In the present paper, a series of sulphided lithium–manganese spinels were prepared by the sol-gel method. The obtained samples, $LiMn_2O_{4-y}S_y$ with different sulphur content, were studied using XRD, MS-TGA, and DSC in relation to their influence on electrical properties. The results are discussed with reference to the properties of stoichiometric $LiMn_2O_4$.

2. Experimental

A set of sulphided lithium–manganese spinels $LiMn_2O_{4-y}S_y$ ($0.09 \leq y \leq 0.5$) was prepared by a modified sol-gel method [17] using solutions of CH_3COOLi, $(CH_3COO)_2Mn$, $(NH_4)_2S$, and concentrated ammonia as the alkalising agent. The synthesis was performed under a constant argon flow to prevent uncontrolled oxidation of Mn^{2+} ions. Condensation of the formed sol was performed at 90 °C for 2 days, and then the obtained xerogel was decomposed in air for 24 h at 300 °C with a heating rate of 1 °C/min. The obtained residue was reground in an agate mortar, providing a brown-black powder. Additional high-temperature calcination (800 °C for 24 h in air), followed by quenching, was performed to obtain better crystallised samples. The nominal compositions and preparation conditions of the obtained samples are presented in Table 1.

The crystal structure of the samples was examined by X-Ray powder diffraction on a PW3710 Philips X'Pert apparatus using $CuK_{\alpha 1}$ radiation (λ = 0.154178 nm) with a graphite monochromator. The phase analysis of the XRD patterns was performed by the Rietveld method using PDF-2 standards and the DBWS-9411 software package [18].

MS-TGA experiments were performed in Mettler-Toledo 851^e microthermobalance in 150 μl open platinum crucibles under a flow of air (60ml/min) within the temperature range 30–1200–30 °C. Evolved gas analysis (EGA) was performed simultaneously by a joined on-line quadruple mass spectrometer (Thermostar-Balzers).

Table 1. Nominal composition and preparation conditions of the sulphided spinel samples

Sample	Nominal composition	Preparation
S 9	$LiMn_2O_{3.91}S_{0.09}$	sol-gel method, condensation and drying at 90 °C, 48 h, calcination in air at 300 °C for 24 h
S 20	$LiMn_2O_{3.8}S_{0.2}$	
S 30	$LiMn_2O_{3.7}S_{0.3}$	
S 40	$LiMn_2O_{3.6}S_{0.4}$	
S 50	$LiMn_2O_{3.5}S_{0.5}$	
QS 9	$LiMn_2O_{3.91}S_{0.09}$	sol-gel method, condensation and drying at 90 °C, 48 h, calcination in air at 300 °C for 24 h, recalcination in air at 800 °C for 24 h then quenching
QS 20	$LiMn_2O_{3.8}S_{0.2}$	
QS 30	$LiMn_2O_{3.7}S_{0.3}$	
QS 40	$LiMn_2O_{3.6}S_{0.4}$	
QS 50	$LiMn_2O_{3.5}S_{0.5}$	

DSC experiments were performed in a Mettler-Toledo 821^e calorimeter, equipped with a Haake intracooler, in 40 μl aluminium crucibles under the flow of argon (80 ml/min) within the temperature range from –40 to 60 °C.

Electrical conductivity was measured using a four-probe AC method at 33 Hz within the temperature range from –20 to 50 °C. To improve the electrical contact, a silver paste with acrylic resin was used.

3. Results and disscussion

Powder diffraction patterns of the obtained sulphided lithium–manganese spinels are presented in Figure 1. The diffraction peaks for the samples (S9, S30, and S50) calcined at 300 °C are broad and of low intensity, typical of defected spinels obtained at low temperatures [17]. Additional calcination at 800 °C provides much better crystallized samples, with narrower and more intensive XRD peaks.

In Table 2, the results of the phase analysis performed using the Rietveld method are presented. For the low-temperature samples, the best fit to XRD patterns was achieved using a two-phase system: spinel (*Fd*3*m*) and hausmannite – Mn_3O_4 (*I*4/*amd*). The amount of spinel phase decreases with increasing sulphur content, simultaneously the lattice constant *a* for this phase increases above the value for the sulphur-free
Li–Mn spinel ($Li_{0.96}Mn_{1.92}O_4$) obtained at 300 °C, namely a = 8.1731 Å [10]. This is in accordance with the substitution of oxygen by larger sulphur anions. Sample QS9 ($LiMn_2O_{3.91}S_{0.09}$) shows only the spinel phase XRD-peaks with the lattice constant a = 8.2630 Å. This value is much higher than that for stoichiometric $LiMn_2O_4$ (a = 8.2517 Å) [10].

Samples calcined at 800 ºC and containing larger amounts of sulphur (QS30 and QS50) showed XRD patterns that need a two-phase system for fitting, with spinel (*Fd*3*m*) and bixbyite (*Ia*3) phases. The amount of spinel phase decreases with increasing sulphur content. Additionally, the bixbyite phase (Mn_2O_3) shows another Li:Mn

stoichiometry, which causes the appearance of lithium excess in the spinel phase. Such a Li-rich spinel phase should reveal a lower lattice constant, which is in fact observed (Table 2). The same influence of lithium excess was previously observed for so called δ-spinels ($Li_{1+\delta}Mn_{2-\delta}O_4$) [10, 11]. For samples with the highest sulphur content (S30, QS30, S50, QS50), a small amount (less than 3%) of $Li_2SO_4 \cdot H_2O$ was observed (peaks around 21.5° and 25°). This is consistent with the mass lost due to dehydration, observed on TG curves (30–100 °C).

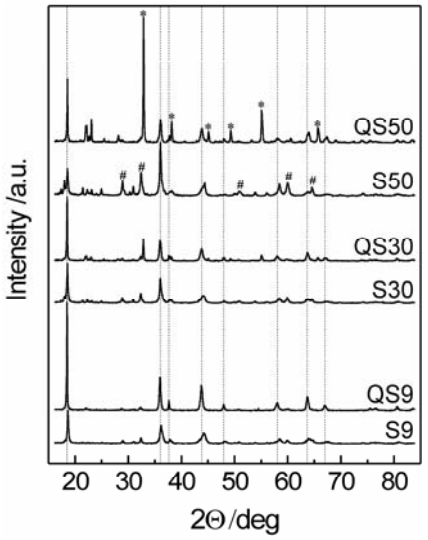

Fig. 1. XRD patterns of sulphided lithium–manganese spinels:
* – Mn_2O_3 bixbyite phase, # – Mn_3O_4 hausmannite phase

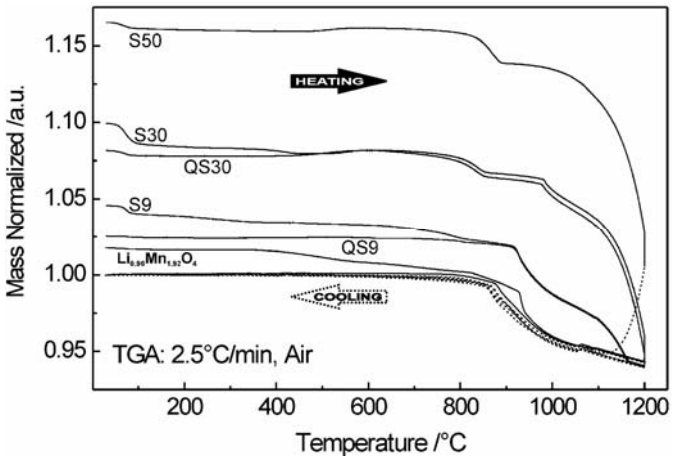

Fig. 2. Thermogravimetric analysis of sulphided lithium–manganese spinels

Table 2. Phase analysis of sulphided Li–Mn spinels

Sample	Nominal composition	Phase analysis
S 9	$LiMn_2O_{3.91}S_{0.09}$	76% spinel (a = 8.2136 Å) 24% hausmannite (a = 5.7573 Å, c = 9.4427 Å)
S 30	$LiMn_2O_{3.7}S_{0.3}$	54% spinel (a = 8.2272 Å) 46% hausmannite (a = 5.7615 Å, c = 9.4259 Å)
S 50	$LiMn_2O_{3.5}S_{0.5}$	29% spinel (a = 8.2356 Å) 71% hausmannite (a = 5.7640 Å, c = 9.4118 Å)
QS 9	$LiMn_2O_{3.91}S_{0.09}$	100% spinel (a = 8.2630 Å)
QS 30	$LiMn_2O_{3.7}S_{0.3}$	75% spinel (a = 8.2413 Å) 25% bixbyite (a = 9.4063 Å)
QS 50	$LiMn_2O_{3.5}S_{0.5}$	35% spinel (a = 8.2443 Å) 65% bixbyite (a = 9.4086 Å)

The results of thermogravimetric analysis (MS-TGA) are presented in Figure 2. The TG curves were recorded in dry air during heating up to 1200 °C and cooling to 30 °C. The TG curve for $Li_{0.96}Mn_{1.92}O_4$ has been added to compare with the curves for sulphur-free samples. Evolved gas analysis (EGA), performed simultaneously with TG measurements, proved that the sulphided spinel loses sulphur as SO_2 above 1000 °C (Fig. 3). The total process of the thermal decomposition of sulphided spinels, $LiMn_2O_{4-y}S_y$ (where $0 < y < 0.5$), may be described by following equation:

$$3LiMn_2O_{4-y}S_y + \left(\frac{9}{2}y - 1\right)O_2 \rightarrow 3LiMnO_2 + Mn_3O_4 + 3ySO_2 \uparrow \qquad (1)$$

It should be stressed that the decomposition product reacts during slow cooling (2.5 °C/min) in air and forms the stoichiometric spinel phase ($LiMn_2O_4$).

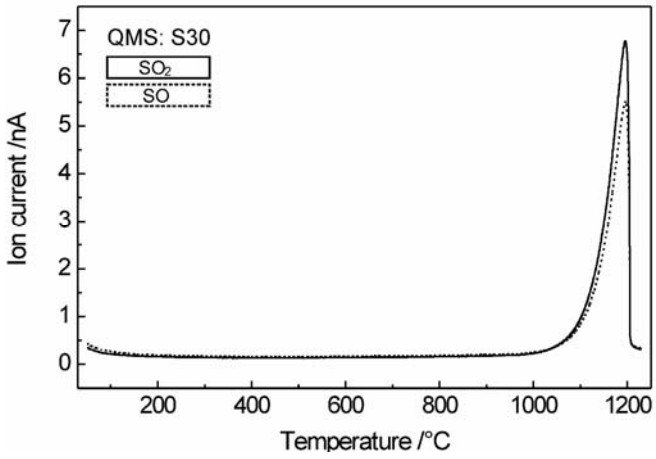

Fig. 3. EGA analysis of sample S30

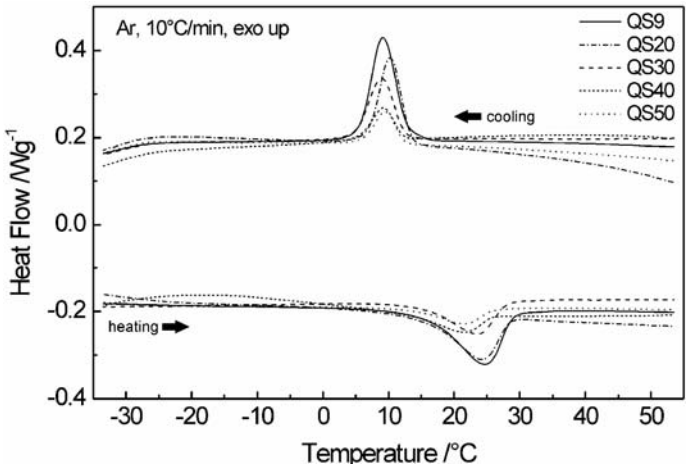

Fig. 4. DSC measurements of the QS-spinels from –30 to 50 °C

DSC measurements of QS samples near room temperature (from –30 to 50 °C) are presented in Figure 4. The thermal effects observed during cooling and heating on DSC curves are related to the phase transition from a cubic to orthorhombic structure. The measured enthalpies (ΔH) of this transformation for sulphided lithium –manganese spinels are collected in Table 3. The values are lower than that for the stoichiometric $LiMn_2O_4$, and they decrease with increasing sulphur concentration. This may suggest structural stabilisation owing to sulphur substitution.

Table 3. Enthalpies ΔH [J/g] of transformation for sulphided lithium–manganese spinel

Sample	Transition around	
	10–25 °C	540–580 °C
$LiMn_2O_4$	8.6	no heat effects
QS 9	6.5	7.0
QS 20	4.8	13.0
QS 30	3.9	24.3
QS 40	1.9	33.0
QS 50	1.7	42.1

The sulphided lithium–manganese spinels calcined at 800 °C reveal another reversible phase transition (with hysteresis about 40 °C) at very high temperatures, which was not observed for the sulphur-free $LiMn_2O_4$ phase (Fig. 5). The measured heat effects are collected in Table 3. This high temperature transformation intensifies with sulphur content. This is a first order phase transition, which needs additional XRD studies in order to explain its nature.

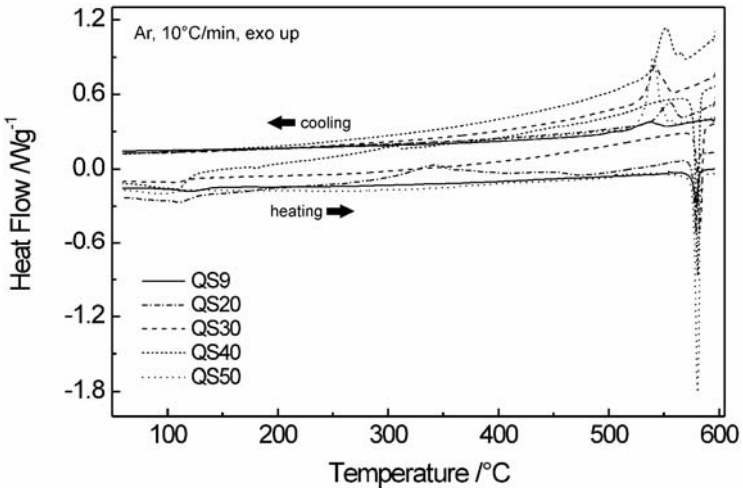

Fig. 5. DSC measurements of the QS-spinels within 25–600 °C

Measurements of the electrical conductivity of sulphided lithium–manganese spinels calcined at 800 °C are presented in Figure 6. The samples calcined at 300 °C reveal low electrical conductivity with a small activation energy (E_a = 0.13–0.28 eV, in the 10–40 °C temperature range). The calcination of these samples at 800 °C increases their electrical conductivity, but it is decreased with sulphur concentration, though the activation energy of electrical conductivity is slightly diminished (E_a = 0.24–0.30 eV, 10–40 °C). The activation energy for the stoichiometric $LiMnO_4$ is equal to 0.32 eV (10–40 °C). This may be explained by a strong distortion of the spinel network by sulphur substitution and in consequence lowering of Mn-Mn distances.

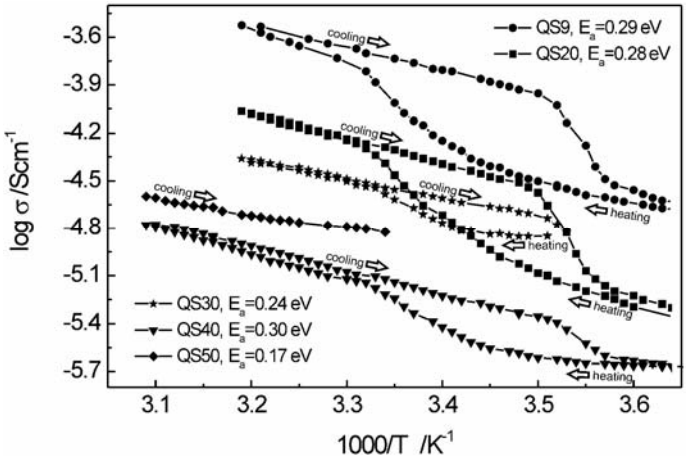

Fig. 6. Electrical conductivity of sulphided lithium–manganese spinels calcined at 800 °C

Data from electrical measurements suggest that the small polaron-conduction mechanism is preserved. The lowering of electrical conductivity with increasing sulphur concentration, which does not change the Mn^{3+}/Mn^{4+} ratio, is most probably caused by a decreasing number of effective carriers. This may suggest that effective electronic transport occurs only through manganese octahedra without sulphur substitution.

4. Conclusions

It is possible to obtain lithium–manganese spinels with partial sulphur substitution in an oxygen lattice. This can be effectively done using the sol-gel technique, followed by calcination at 800 °C in air. The single-phase material was obtained only for concentrations of sulphur less than 0.20 mole per spinel molecule.

The introduction of sulphur into the spinel lattice reduces the phase transition around room temperature, but another one appears at higher temperatures (540–580 °C). The explanation of the nature of the high-temperature transition demands further studies. The sulphided lithium–manganese spinels do not decompose up to 850 °C in air. Above this temperature, the spinels thermally decompose with the simultaneous oxidation of sulphur to SO_2.

The sulphur substitution of oxygen in the spinel lattice lowers electrical conductivity. Assuming the preservation of the small polaron mechanism, one may conclude that hopping is limited only to MnO_6 octahedra. The problem of cycling stability also requires additional studies.

Acknowledgements

The work is supported by the Polish Committee for Scientific Research under grant 3 T08D 010 28. One of the authors (M.M.) would like to acknowledge the Foundation for Polish Science for support in the form of The Annual Stipend for Young Scientists.

References

[1] TARASCON J.M., ARMAND M., Nature, 414 (2001), 359.
[2] WHITTINGHAM M.S., Solid State Ionics, 134 (2000), 169.
[3[AMATUCCI G.G., DU PASQUIER A., BLYR A., ZHENG T., TARASCON J.M., Electrochimica Acta, 5 (1999), 255.
[4] RODRIGUEZ-CARVAJAL J., ROUSSE G., MASQUELIER C., HERVIEU M., Phys. Rev. Lett., 81 (1998), 4660.
[5] YAMADA A., TANAKA M., Mat. Res. Bull., 30 (1995), 715.
[6] YAMADA A., TANAKA M., TANAKA K., SEKAI K., J. Power Sources, 81, 82 (1999), 73.
[7] WU Y.P., RAHM E., HOLZE R., Electrochim. Acta, 47 (2002), 3491.
[8] MOLENDA J., MARZEC J., SWIERCZEK K., OJCZYK W., ZIEMNICKI M., WILK P., MOLENDA M., DROZDEK M., DZIEMBAJ R., Solid State Ionics, 171 (2004), 215.
[9] CAPSONI D., BINI M., CHIODELL G., MASSAROTTI V., MUSTARELL P., LINATI L., MOZZATI M.C., AZZONI C.B., Sol. State Comm., 126 (2003), 169.

[10] DZIEMBAJ R., MOLENDA M., J. Power Sources, 119–121C (2003), 121.
[11] SWIERCZEK K., MARZEC J., MARZEC M., MOLENDA J., Solid State Ionics, 157 (2003), 89.
[12] MOLENDA M., DZIEMBAJ R., PODSTAWKA E., PRONIEWICZ L.M., J. Phys. Chem. Solids, 66 (2005), 1761.
[13] PISZORA P., J. Alloys and Compounds, 382 (2004), 112.
[14] SUN Y.K., JEON Y.S., Electrochem. Commun., 1 (1999), 597.
[15] PARK S.H., PARK K.S., SUN Y.K., NAHM K.S., J. Electrochem. Soc., 147 (2000), 2116.
[16] SUN Y.K., LEE Y.-S., YOSHIO M., Mat. Lett., 56 (2002), 418.
[17] DZIEMBAJ R., MOLENDA M., MAJDA D., WALAS S., Solid State Ionics, 157 (2003), 81.
[18] YOUNG R.A., DBWS-9411, Release 30.3.95, School of Physics, Georgia Institute of Technology, USA 1995.

Received 10 December 2004
Revised 13 March 2005